Synthesis of nano-textured biocompatible scaffolds from chicken eggshells

2012 Nanotechnology 23 475601

(http://iopscience.iop.org/0957-4484/23/47/475601)

Nanotechnology **23** (2012) 475601 (9pp) doi:10.1088/0957-4484/23/47/475601

Synthesis of nano-textured biocompatible scaffolds from chicken eggshells

Waseem Asghar[1,2,3,6,7], **Young-Tae Kim**[3,4], **Azhar Ilyas**[1,2,3], **Jeyantt Sankaran**[1,2,3,8], **Yuan Wan**[1,3,4,9] **and Samir M Iqbal**[1,2,3,4,5]

[1] Nano-Bio Lab, University of Texas at Arlington, Arlington, TX 76019, USA
[2] Department of Electrical Engineering, University of Texas at Arlington, Arlington, TX 76011, USA
[3] Nanotechnology Research and Education Center, University of Texas at Arlington, Arlington, TX 76019, USA
[4] Department of Bioengineering, University of Texas at Arlington, Arlington, TX 76010, USA
[5] Joint Graduate Committee of Bioengineering Program, University of Texas at Arlington and University of Texas Southwestern Medical Center at Dallas, University of Texas at Arlington, Arlington, TX 76010, USA

E-mail: smiqbal@uta.edu

Received 8 March 2012, in final form 27 August 2012
Published 30 October 2012
Online at stacks.iop.org/Nano/23/475601

Abstract
Cell adhesion, morphology and growth are influenced by surface topography at nano and micrometer scales. Nano-textured surfaces are prepared using photolithography, plasma etching and long polymer chemical etching which are cost prohibitive and require specialized equipment. This article demonstrates a simple approach to synthesize nano-textured scaffolds from chicken eggshells. Varieties of pattern are made on the eggshells like micro-needle forests and nanopores, giving very uniform nano-textures to the surfaces. The surfaces are characterized for chemical composition and crystal phase. The novel patterns are transferred to PDMS surfaces and the nano-textured PDMS surfaces are used to study the effect of texturing on human fibroblast cell growth and attachment. The effects of surface topographies, along with laminin coating on cell cultures, are also studied. We find an exciting phenomenon that the initial seeding density of the fibroblast cells affects the influence of the nano-texturing on cell growth. These nano-textured surfaces give 16 times more fibroblast growth when compared to flat PDMS surfaces. The novel nano-textured patterns also double the laminin adsorption on PDMS.

S Online supplementary data available from stacks.iop.org/Nano/23/475601/mmedia

(Some figures may appear in colour only in the online journal)

1. Introduction

Many studies show that cell growth, adhesion and orientation are influenced by the surface features of the substrates like pores, fibers and ridges at nanometer dimensions [1, 2]. Cell attachment and proliferation are improved on textured surfaces when compared to flat ones [3, 4]. Basement membranes are found throughout the human body and serve as an underlying layer for cellular structures. The basement membrane consists of extracellular matrix (ECM) which includes fibrous collagen, proteoglycans, fibronectin, hyaluronic acid and laminin. The ECM structure is nanoporous with a collagen fibrous network. Substrates having nano-structures, dense nanopores and a high surface area are considered ideal in many tissue engineering applications because of the topographical resemblance to ECM [5–7]. Therefore, a process to make surfaces with

[6] Present address: Harvard-MIT Division of Health Sciences and Technology, Massachusetts Institute of Technology, Cambridge, MA 02139, USA.
[7] Present address: Center for Biomedical Engineering, Department of Medicine, Brigham and Women's Hospital, Harvard Medical School, Boston, MA 02115, USA.
[8] Present address: College of Engineering and Applied Sciences, Stony Brook University, Stony Brook, NY 11794, USA.
[9] Present address: Mawson Institute, University of South Australia, Adelaide, Australia.

nano-texturing is highly desirable. Secondly, textured surfaces have found many applications in biosensors, proteomics and light emitting diodes [8–12]. One of the key features offered by nano-textured surfaces is their increased surface area, which allows an increased quantity of protein or nucleic acid binding to capture specific biological targets [13]. Nano-textured surfaces are prepared using photolithography, plasma etching, micro-contact printing, stencil assisted patterning and long polymer chemical etching processes which are cost prohibitive or require special equipment [2, 14]. Therefore, a simple and cost-effective fabrication process is required to make nano- and micro-textured surfaces.

We report a simple and inexpensive approach to make three-dimensional nano- and micro-structures using chicken eggshell. Chicken eggshell (calcite, coralline calcium carbonate) is totally resorbable and biocompatible with good osteoconductivity [15–17]. Calcium carbonate has emerged as a novel bone substitute in its natural form or its derived form, hydroxyapatite (HA) or calcium sulfate, for bone healing in dentistry and orthopedics [18–21]. Eggshells have previously been used to synthesize nanoparticle apatite and HA nano-powder that requires sintering to make porous scaffolds [22–24]. However, eggshells can provide novel substrate features that can be tailored for many more applications. For the first time, we report the synthesis of nano-textured scaffolds by wet chemical etching of chicken eggshells. Briefly, chicken eggshells are treated with diluted hydrochloric acid (HCl) and sulfuric acid (H_2SO_4) to make nanoporous and eggshell-grass scaffolds respectively. The patterns are successfully transferred to polydimethylsiloxane (PDMS). The PDMS scaffolds are then used to study the influence of nano-texturing on the growth of human fibroblast cells.

2. Materials and methods

All chemicals were obtained from Sigma-Aldrich (St Louis, MO) unless otherwise noted.

2.1. Synthesis of eggshell scaffold

Chicken eggs were purchased from a grocer (Walmart). These were white, cage-free and omega-3 eggs supplied by Great Day Farms. A total of six eggs were used in the experiments. The chicken eggshells were cleaned from inside by boiling for 30 min in hot water. The eggshells were then washed with deionized (DI) water followed by drying in nitrogen flow. In order to make nanoporous scaffolds, the eggshells were dipped in 15% HCl for 5 min. The HCl-treated eggshells were washed with copious amounts of DI water and dried with nitrogen. In order to make micro-needle scaffolds (eggshell-grass scaffolds), the eggshells were dipped in 25% H_2SO_4 for 30 min. The H_2SO_4-treated eggshells were also washed with a copious amounts of DI water and dried with nitrogen. The final scaffolds were stored in Petri dishes.

2.2. Gold coating for SEM imaging

For scanning electron microscope (SEM) imaging, a 40 Å thin film of gold was sputtered on eggshell samples to make these conductive for SEM imaging, while 150 Å gold film was used on cell samples (figure 8). The SEM (ZEISS Supra 55) was used in variable pressure mode. A secondary electron detector at high vacuum was used for SEM imaging.

2.3. Energy-dispersive x-ray spectroscopy and mapping

Energy-dispersive x-ray spectroscopy (EDS) was used for elemental analysis of eggshell scaffolds. An EDS detector (EDAX, Genesis) was attached to the SEM. After loading the sample, the SEM was focused at a 15 mm working distance with 15 kV applied voltage. EDS data were recorded followed by mapping analysis.

2.4. X-ray diffraction analysis

X-ray diffraction (XRD) analysis was performed using a KristalloFlex-810, Siemens D-500 System. X-ray diffraction data were captured under the following conditions: 2θ_start = 8°, 2θ_end = 120°, step size = 0.05 and dwell time = 3 s.

2.5. PDMS templating

The eggshell scaffolds were treated with 1*H*,1*H*,2*H*,2*H* perfluorooctyl-trichlorosilane (PFTS). The thin film coating of PFTS helped in peeling the PDMS (Sylgard 184, Dow Corning) off the scaffolds [25]. For PFTS application, the eggshell scaffolds were put on a hot plate next to a glass slide that carried a few drops of PFTS. These were covered with a glass Petri dish with a small hole in it. The temperature of the hot plate was raised to 250 °C. The PFTS evaporated and deposited on the eggshells scaffolds making a few nm polymer layers [26]. The eggshell scaffolds were removed after 20 min and allowed to cool down. The PDMS was prepared by mixing the base curing agent at a ratio of 1:10 [27]. All the air bubbles were removed by putting PDMS in a vacuum chamber. The PDMS was then poured on the eggshell scaffolds and allowed to polymerize for 10 min at 150 °C. The samples were cooled down and the PDMS was peeled off the eggshells.

2.6. AFM analysis

An atomic force microscope (AFM; Park Systems., Santa Clara, CA, USA) was used for surface analysis of the PDMS scaffolds. Non-contact tips (NCLR f^o: 190 kHz, C: 48 N m^{-1}, NanoWorld AG) were used to analyze the PDMS surface.

2.7. Human-derived primary immortalized fibroblast cell culture

Human fibroblast cells were obtained from consenting patients at the University of Texas Southwestern Medical Center (Dallas, TX, USA) with the approval of the Institutional Review Board. The collected human fibroblast cells were cultured in Dulbecco's modified Eagle's medium (DMEM/F-12, Cellgro, Mediatech Inc.) with 10% fetal

bovine serum. Gentamycin and L-glutamine (Invitrogen) were also added to the cell culture medium. The cells were incubated under standard cell culture conditions i.e. a sterile, humidified, 95% air, 5% CO_2 and 37 °C environment.

2.8. In vitro cell culture studies on nano-textured PDMS scaffolds and laminin coating

The PDMS scaffolds (plain and nano-textured) were cut into 6 mm diameter circular disks. All the scaffolds were glued into a 24-well plate using UV glue (Dymax Corporation). The well plate was left under a UV lamp for 20–30 min to cure the UV glue. All the PDMS scaffolds were washed three times with DI water and dried in nitrogen flow. The plate was then treated with O_2 plasma for 30 min to sterilize the scaffolds. The plasma treatment also made the surface of the PDMS hydrophilic. All of the scaffolds were thoroughly washed again with DI water three times. The samples were then coated with poly-D-lysine (PDL) by immersing the scaffolds in PDL solution for 24 h. The wells were washed again with sterilized DI water three times. The samples were then coated with laminin by immersing the samples in a solution with 10 μg ml^{-1} laminin in 1× PBS (PBS was Mg^{+2}/Ca^{+2} free). The well plate was kept at 37 °C in an incubator for 3–4 h to adhere laminin to the PDMS surfaces [28]. The laminin solution was then removed from the wells and the samples were washed with sterilized 1× PBS three times. Freshly harvested human fibroblasts (in cell culture medium) were seeded onto the PDMS samples (4000 cells cm^{-2} for low density cell culture studies or 100 000 cells cm^{-2} for high density cell culture studies). Four samples were prepared for each condition ($n = 4$). Statistical analysis was performed using one-way ANOVA for three independent samples.

2.9. Immunostaining of human fibroblast cells

After cell culture for three days, the cell culture medium was removed from the wells. The cells were fixed by immersing them into 4% paraformaldehyde for 3 h. In order to prepare a blocking solution, goat serum was mixed with washing solution (0.5% Triton X-100 in 1× PBS solution) to make 4% goat serum. After 3 h, the 4% paraformaldehyde was removed and the cells were washed three times with 1× PBS, and blocking solution was added to samples for 1 h at room temperature. The blocking solution was replaced with primary antibody solution (Vimentin, mIgG1, 1:500) and the well plate was left overnight at 4 °C. The next day, the primary antibody solution was removed and all the samples were washed three times with washing solution. The secondary antibody solution was prepared by mixing goat anti-mouse IgG_1 Dylight 488 (Jackson ImmunoResearch Laboratories Inc., USA) with washing solution (1:4000). The secondary antibody solution was added to all wells after washing the samples. The samples were left for 1 h at room temperature. The samples were then washed three times with washing solution and 1× PBS was added at the end. All the samples were imaged with a fluorescence microscope.

2.10. Laminin adsorption on nano-textured PDMS

The method to stain for laminin was similar to the immunostaining method for the fibroblasts, except different primary and secondary antibodies were used. After fixing the laminin adsorbed on the different surface types with 4% paraformaldehyde, primary laminin antibody (rabbit IgG, 1:200) was added to all of the wells and kept at 4 °C overnight. Then the primary solution was removed and the secondary antibody solution, goat anti-rabbit IgG Dylight 488 (1:400, Jackson ImmunoResearch Laboratories Inc.), was added and the well plate was kept at room temperature for 1 h. After washing with buffer, 1× PBS was added. All the samples were imaged using a fluorescence microscope under the same exposure conditions. Four images were taken for each sample from random parts. The intensity data were measured and quantified with *ImageJ* software. The intensities were calculated by selecting random areas of the images avoiding very bright spots. Statistical analysis was performed using one-way ANOVA for three independent samples.

2.11. Cell sample preparation for SEM analysis

In order to prepare the cell samples for SEM analysis, different ethanol gradient solutions (v/v) were prepared by mixing with DI water at concentrations of 20%, 30%, 50%, 70%, 85%, 95% and 100% [13]. The gradient solutions were used to remove water from the cells that helped the cells to be fixed without rupturing the cell walls. The cells were first fixed by immersing them in 4% paraformaldehyde for 1 h. All the samples were then put in each ethanol gradient solution for 15 min in order of increasing concentration (starting with 20%). The samples were stored at −20 °C overnight. The samples were sputtered with 15 nm of gold layer followed by SEM imaging.

3. Results and discussions

3.1. Chemical treatment of eggshells

The eggshell samples were cleaned as described in the materials and method section. When the samples were treated with diluted HCl and H_2SO_4, different nano-textures were produced on the eggshell surface. The SEM micrographs (figures 1(a)–(c)) show that chemically treated eggshell samples had nano-features and micro-needles. The SEM micrographs also reveal that the native and untreated eggshell does not have grass-like micro-features or a nanoporous texture on the surface. On the other hand, H_2SO_4-treated scaffolds show needles with widths ranging between 500 nm–3 μm and the lengths of most of the needles are 50 μm (supplementary figure 1 available at stacks.iop.org/Nano/23/475601/mmedia). These eggshell micro-needles are similar to silicon grass in shape [29, 30]. The concentration of sulfuric acid was changed to 50% and 75%, but it did not have any effect on the final size, shape, orientation, thickness or length of the micro-needles. The concentrated acid increased the rate of chemical reaction with no differences in the final features of the micro-needles.

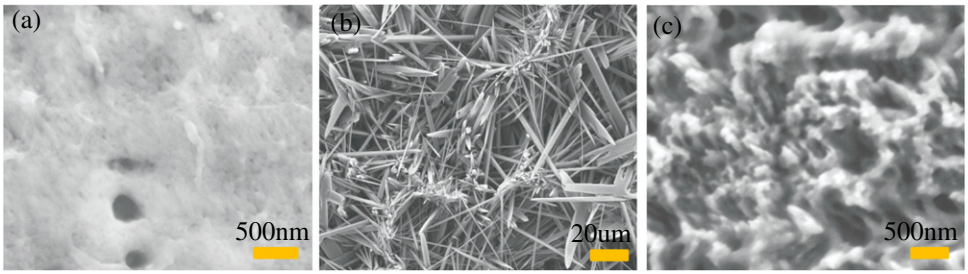

Figure 1. SEM micrographs for native untreated and chemically treated eggshell surfaces. (a) Untreated eggshell surface. (b) Eggshell treated with 25% H_2SO_4 solution for 30 min. (c) Eggshell treated with 15% HCl solution for 5 min.

When the eggshells were treated with diluted HCl, a nanoporous texture was formed on the surface. The diameter of the average nanopore was less than 100 nm (supplementary figure 2 available at stacks.iop.org/Nano/23/475601/mmedia). The pattern was very uniform over the whole surface. Other concentrations of HCl (25%, 50%) were also used but, again, these showed only an increase in the chemical reaction with no differences in the final texture. On the other hand, with concentrations of HCl, it was difficult to control the chemical reaction as the HCl reacted vigorously with the chicken eggshell.

3.2. EDS elemental analysis and compositional mapping

To analyze the material composition, energy-dispersive x-ray spectroscopy (EDS) was performed. EDS elemental analysis showed that the original chicken eggshell mainly consisted of Ca, C, O, P and Mg as shown in figure 2(a). The EDS spectrum showed that the carbon content decreased significantly in H_2SO_4-treated samples as the carbon would form CO_2 during the chemical reaction (figure 2(b)). Secondly, some organic impurities might also have been dissolved during the chemical reaction. The decrease of carbon and the appearance of sulfur content were due to the chemical reaction as shown by equation (1).

$$CaCO_3 + H_2SO_4 \rightarrow CaSO_4 + H_2O + CO_2. \quad (1)$$

Eggshell mainly consists of calcium carbonate (94%), calcium phosphate (1%), organic matter (4%) and magnesium carbonate (1%) [31, 23, 32]. When calcium carbonate reacted with sulfuric acid, needle-like features were formed which were assumed to be made up of calcium sulfate. The composition mapping was performed on the H_2SO_4-treated sample as explained in the materials and methods section (also supplementary figure 3 available at stacks.iop.org/Nano/23/475601/mmedia). It is evident that calcium was abundantly present all over the sample but oxygen and sulfur were mainly present on the surface of the micro-needles. This was due to the fact that the native and untreated eggshell is made up of calcium carbonate which has calcium everywhere. Thus, the bottom surface might still have calcium carbonate. However, it is clear that sulfur was only present on the needle surface, which proved the formation of calcium sulfate crystals in the processed sample. Carbon was also present in a few areas, probably due to the presence of underlying calcium carbonate which was still in its original form.

In the case of the eggshell reaction with diluted HCl, again the carbon content was reduced (figure 2(c)). This was due to the release of CO_2 and dissolution of organic components during the chemical reaction. Chlorine did not appear in the EDS spectrum, because $CaCl_2$ precipitated out in the solution. The reaction equation of eggshell with HCl is given by equation (2).

$$CaCO_3 + 2HCl \rightarrow CaCl_2 + H_2O + CO_2. \quad (2)$$

The appearance of the nano-features on the eggshell surface was due to non-uniform etching of the eggshell surface. When HCl was reacting with eggshell, CO_2 was being released at the same time and bubbles were formed. The bubbles prevented the physical contact between certain areas of the eggshell surface and HCl for a specific time. This bubble prevention process allowed the uneven chemical etching of the eggshell surface which led the surface to have nano-features at the end. In this case, the eggshell material did not dramatically change to other compounds like the formation of calcium sulfate that happened in the case of H_2SO_4 etching.

3.3. XRD crystal analysis

The eggshell samples were also characterized with XRD (figure 3). *Jade*5 software was used to analyze the XRD data. It was found that native eggshells showed a significant peak around $2\theta \sim 30°$ which was characteristic of crystalline calcite having *hkl* (104) [33]. The results were in accordance with previous reports [34]. The XRD spectrum of H_2SO_4-treated eggshell clearly showed that there were few peaks which were not associated with calcite (denoted by stars in figure 3(a)). These peaks were characteristic for calcium sulfate dihydrate (CSD) crystals [35]. These three peaks ($2\theta \sim 12°$, 20° and 24°) are similar to those reported earlier for CSD crystals [35]. The overlapping of two XRD spectra, in different regions, might be due to the fact that the calcite phase was still present in the underlying layers (figure 3(a)). The sample treated with HCl showed an XRD spectrum very similar to that of the original eggshell (figure 3(b)). The XRD spectra of both of the samples (original eggshell and HCl-treated) perfectly overlapped with a significant peak around $2\theta \sim 30°$ (calcite crystalline phase). The HCl just

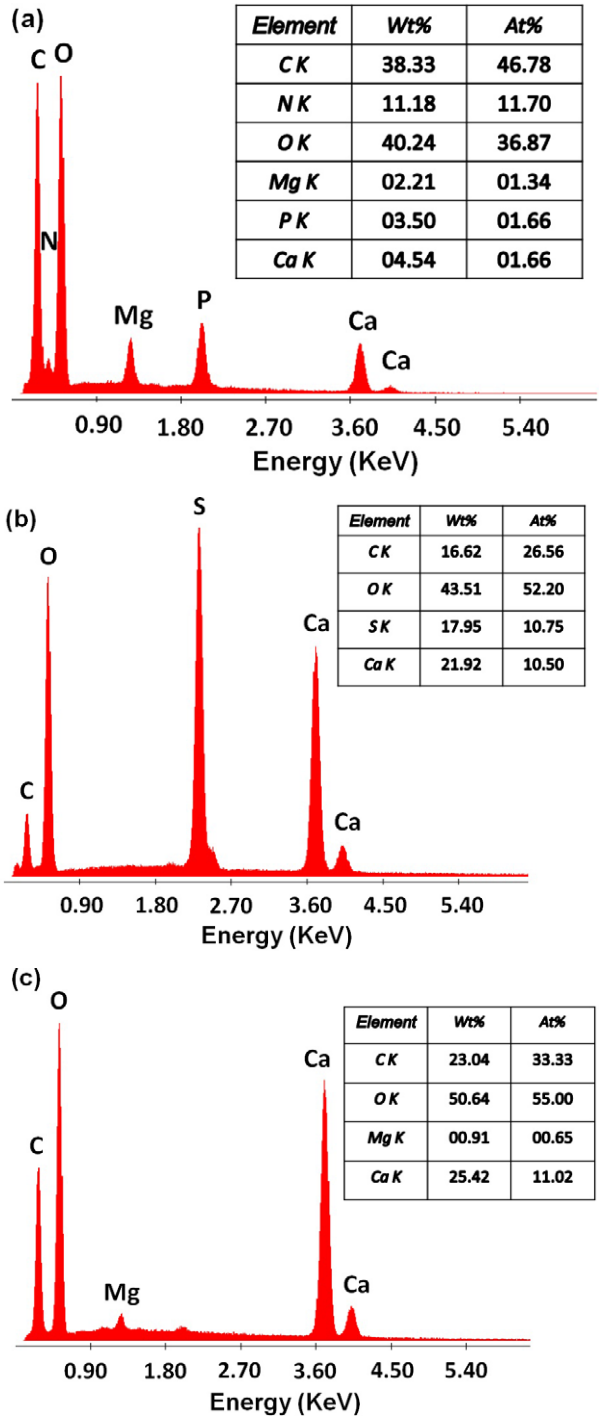

Element	Wt%	At%
C K	38.33	46.78
N K	11.18	11.70
O K	40.24	36.87
Mg K	02.21	01.34
P K	03.50	01.66
Ca K	04.54	01.66

Element	Wt%	At%
C K	16.62	26.56
O K	43.51	52.20
S K	17.95	10.75
Ca K	21.92	10.50

Element	Wt%	At%
C K	23.04	33.33
O K	50.64	55.00
Mg K	00.91	00.65
Ca K	25.42	11.02

Figure 2. EDS elemental analysis of untreated and chemically treated eggshell samples. (a) EDS spectrum of native eggshell without any chemical treatment. (b) EDS spectrum of an eggshell sample treated with diluted H_2SO_4. (c) EDS spectrum of an eggshell sample treated with diluted HCl.

etched the surface but did not change the surface composition, as also seen in EDS analysis.

3.4. Polymer casting and surface analysis

PDMS was cast onto the chemically treated eggshells as explained in the materials and methods section. A nanolayer of PFTS polymer was deposited before casting the PDMS, as PFTS helps in peeling the cured PDMS off the surface. The thickness of the PFTS was expected to be a few nanometers, in line with earlier reports [25, 36]. Three different samples were synthesized i.e. PDMS cast from a plain glass surface (Sample-1), PDMS cast from eggshell with micro-needles (Sample-2) and PDMS cast from nano-textured eggshells (Sample-3). For convenience we will use Sample-1 (plain control), Sample-2 (cast from H_2SO_4-treated eggshell) and Sample-3 (cast from HCl-treated eggshell) in the remaining text. All the PDMS samples were analyzed using an AFM. The AFM micrographs revealed that Sample-2 showed both micro and nano-features while Sample-3 had only nano-features (figure 4). For Sample-2, the micro-features were transferred from the micro-needles. As the micro-needles were very dense, there were nano-gaps present between the micro-needles which resulted in the presence of nano-features on Sample-2. The samples were further analyzed with SEM (supplementary figure 4 available at stacks.iop.org/Nano/23/475601/mmedia). SEM micrographs clearly showed that Sample-2 had variable size features ranging from the nanometer to micron scale. A very uniform nano-texture was observed on the surface of Sample-3 (supplementary figure 4 available at stacks.iop.org/Nano/23/475601/mmedia).

3.5. Laminin coating on PDMS samples

In order to study the *in vitro* cell growth on different surfaces, human fibroblast cells were seeded onto the PDMS samples without laminin coating. The cells were grown for three days. It was observed that the cells were not growing well on the PDMS surfaces, as the intrinsic hydrophobicity of the PDMS did not allow the cells to attach and form focal contacts. Cells like to grow on moderately hydrophilic surfaces. Cell membrane proteins are found to be highly adsorbed on moderately hydrophilic surfaces which facilitate cell adhesion. It is important to note here that highly hydrophilic surfaces prevent protein adsorption. The flat PDMS surface is very hydrophobic due to the presence of methyl groups on both sides of the backbone chain with an average contact angle of $\sim 115^\circ \pm 2^\circ$. The hydrophobic surfaces are known to become more hydrophobic with nano-texturing, while hydrophilic surfaces become more hydrophilic with nano-texturing [13]. Thus, the nano-texturing would not help in reducing the contact angle of the hydrophobic PDMS surface. The samples were thus coated with laminin to make them hydrophilic as described in the material and methods section [28].

To verify the laminin attachment, we carried out the fluorescence imaging. The fluorescence intensity was measured and quantified on all of the samples (figure 5). The fluorescence intensity showed that the laminin attachment on nano-textured PDMS (Sample-3) was 2 times more than that for flat PDMS (Sample-1) because it had more surface area available for attachment. The results also showed $\sim$50% more protein attachment on the nano-textured PDMS surface (Sample-3) as compared to that on micro-textured PDMS (Sample-2). Statistical analysis one-way (ANOVA) showed

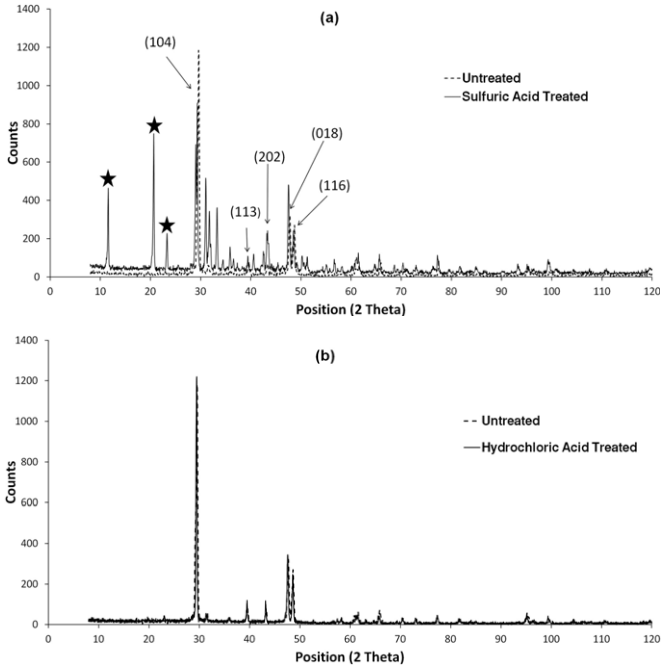

Figure 3. X-ray diffraction spectra for untreated and chemically treated eggshell samples. (a) Comparison between XRD spectra of original eggshell and H_2SO_4-treated eggshell. The peaks represented by arrows show the significant characteristics of the crystalline calcite phase having *hkl* (104), (113), (202), (018) and (116). Stars depict peaks not associated with calcites. (b) Comparison between XRD spectra of original eggshell and HCl-treated eggshell.

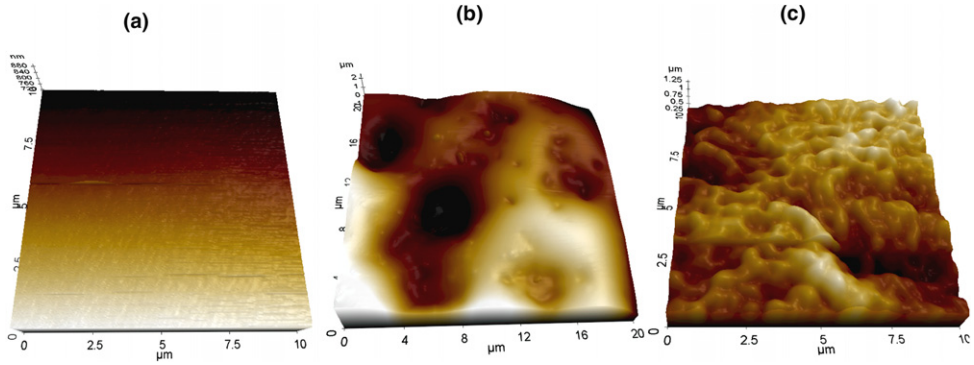

Figure 4. AFM micrographs of PDMS sample. (a) Sample-1, PDMS cast on a plain glass surface. (b) Sample-2, PDMS cast on eggshell with micro-needles. (c) Sample-3, PDMS cast from nano-textured eggshell surface.

that there were significant differences between Sample-1, Sample-2 and Sample-3 (P-value < 0.0001, $n = 4$, figure 5).

3.6. In vitro cell growth on nano-textured surfaces

Human fibroblast cells were then seeded on the three types of PDMS substrates after laminin coating. The cell growth was significantly more on laminin coated textured Sample-2 and Sample-3 as compared to laminin coated plain Sample-1 (figure 6). The cell density also increased from 63 ± 14 cells mm^{-2} (Sample-1) to 810 ± 207 cells mm^{-2} (Sample-2) and 1035 ± 130 cells mm^{-2} (Sample-3) (figure 7). The PDMS samples cast from HCl-treated eggshell showed denser and uniform cell growth compared to other PDMS samples. One-way ANOVA showed that there were statistically significant differences (P-value < 0.01) between Sample-1 and the other samples. Although Sample-3 had a higher cell density, it was not significantly different from Sample-2 (P-value = 0.1236). It was also observed that if the initial cell seeding density was increased from 4000 cells cm^{-2} to 100 000 cells cm^{-2}, the effects of nano-texturing on cell growth faded out. The cells proliferated well on Sample-1 also, although these were fewer in number compared to other samples. A similar cell seeding number effect on MDCK epithelial cell growth has been reported previously [37]. Cell–cell contact might have given rise to increased directed mechanical forces between cells during dense cell culture [28]. The decreased topographical effect on the cell growth might have resulted from these mechanical forces.

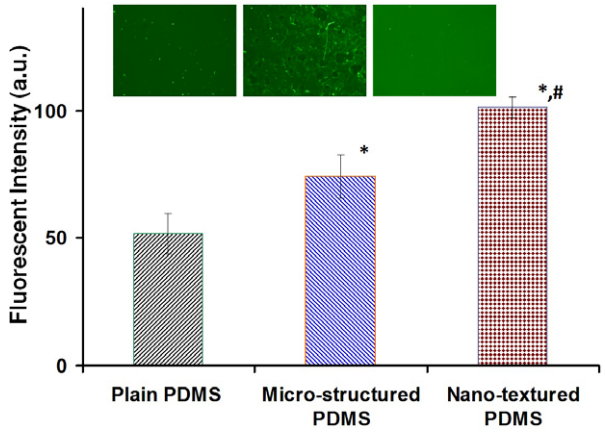

Figure 5. The fluorescence intensity (a.u.) after laminin coating of PDMS samples. (Left inset) PDMS sample casted from a plain glass surface (Sample-1). (Middle inset) PDMS samples casted from eggshell having micro-needles (Sample-2). (Right inset) PDMS sample casted from eggshell having nano-texture (Sample-3). Laminin adsorbed on the different surface types is fluorescently labeled by immunohistochemical analysis. There were significant statistical differences between the plain and textured PDMS samples ($*p < 0{:}0001$, $n = 4$). Nano-textured PDMS (Sample-3) samples were also statistically different from micro-structured PDMS (Sample-2) samples ($\#p < 0{:}0001$; $n = 4$).

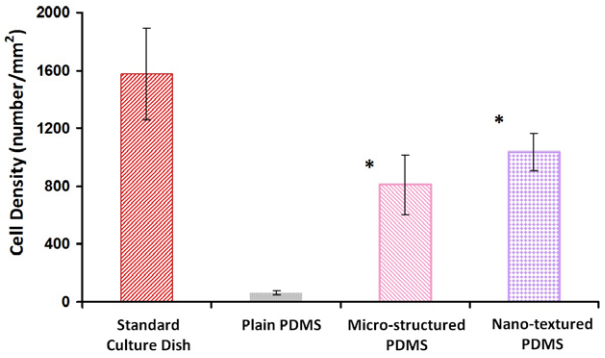

Figure 7. Comparison of cell growth studies on textured and plain PDMS surfaces. The human fibroblast density increased on the nano-textured PDMS surface as compared with the plain PDMS surface. The cells were imaged and counted after three days of cell proliferation. There were significant statistical differences between plain PDMS (Sample-1) and the other samples ($*p < 0{:}01$; $n = 4$). On the other hand, micro-structures (Sample-2) and nano-textured (Sample-3) surfaces were not statistically different ($\#p = 0{:}1236$; $n = 4$).

3.7. Cell morphology on nano-textured PDMS

Distinct differences in cell morphology were also evident between the flat and nano-textured PDMS surfaces. The cells on the flat PDMS surface were spherical in shape (figure 8), while cells on the nano-textured surfaces were elongated and well-spread. We believe that the nano-texturing allows the cells to better attach on the surface and helps in their growth. SEM micrographs showed that fibroblast cells were $\sim$100 μm elongated on the nano-textured PDMS surface while cells on the plain PDMS were no more than 30 μm in any dimension.

In this paper, we show that nano-texturing plays a very important role in protein adsorption on substrate, as well as for cell adhesion and proliferation. The nano-textured surfaces offered increased surface area which allowed more protein attachment and finally facilitated cell adhesion and

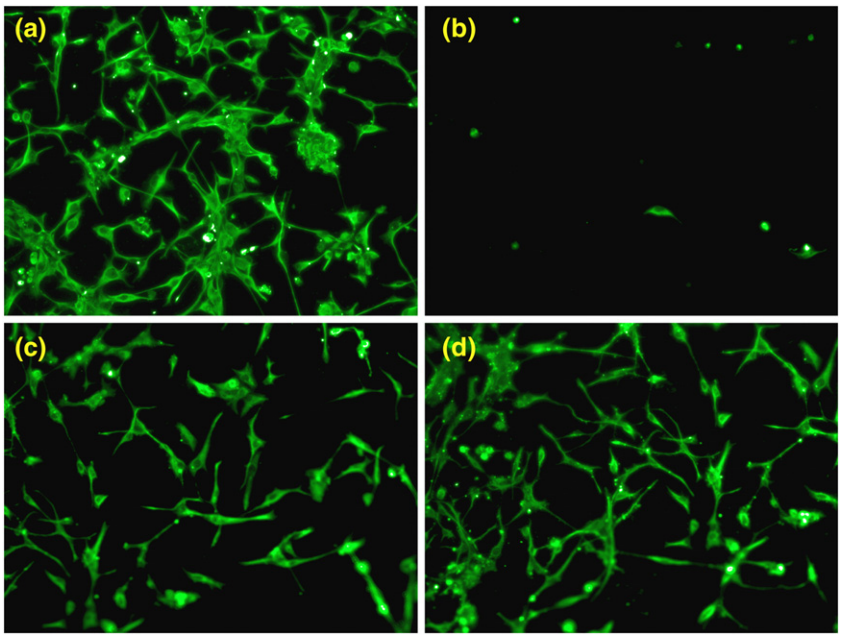

Figure 6. Fluorescently labeled human fibroblasts on different surface types. Cells were cultured for three days before fluorescence imaging. (a) Fibroblast growth in cell culture dish. (b) Fibroblast growth on plain PDMS (Sample-1). (c) Fibroblast growth on micro-structured PDMS (Sample-2). (d) Fibroblast growth on nano-textured PDMS (Sample-3).

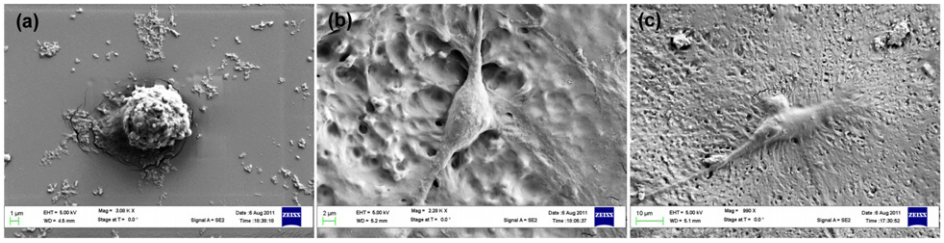

Figure 8. SEM micrographs showing human fibroblast morphology on PDMS surfaces. (a) Cell shape on a flat PDMS sample (spherical). (b) Cell shape on a PDMS sample synthesized from micro-needles (Sample-2, elongated). (c) Cell shape on a PDMS sample synthesized from nano-textured surface (Sample-3, elongated and spread out).

growth. Surface nano-texturing can also play an important role in biosensor applications. In our previous work on nano-textured surfaces, we have seen that such surfaces offer a high degree of surface functionalization. This phenomenon results in a much more dense film of surface-bound epidermal growth factor receptor-specific RNA aptamers, increasing the sensitivity for the capture of tumor cells from cell mixtures [13, 12].

4. Conclusions

We conclude that the reported synthesis method is simple, rapid and cost-effective. As these structures are synthesized from chicken eggshells, it opens a new paradigm to create nano-textured surfaces while recycling common waste. The micro-needle pattern is unique in a way that it resembles silicon grass which has been studied for different applications including cell culture studies. The nano-texture patterns can be successfully transferred to many polymers like PDMS. The nano-textured PDMS allows more protein attachment due to the increased surface area. The growth rate of the cells is higher on these surfaces as compared to flat ones, alluding to the power of nano-textured substrates that can significantly enhance cell culture studies.

Acknowledgments

Partial synthesis, fabrication and characterization were done at the Nanotechnology Research and Education Center (NanoFab), Characterization Center For Materials And Biology (C^2MB) at the University of Texas at Arlington and the Cleanroom Research Laboratory at the University of Texas at Dallas, TX. We also want to thank Deepika Tamuly and Poorva Abhyankar for their help during cell culture. WA and AI were partially supported by a fellowship from the Consortium for Nanomaterials for Aerospace Commerce and Technology (CONTACT) program, Rice University, Houston, TX, USA.

References

[1] Biela S A, Su Y, Spatz J P and Kemkemer R 2009 Different sensitivity of human endothelial cells, smooth muscle cells and fibroblasts to topography in the nano–micro range *Acta Biomater.* **5** 2460–6

[2] Bacakova L, Filova E, Parizek M, Ruml T and Svorcik V 2011 Modulation of cell adhesion, proliferation and differentiation on materials designed for body implants *Biotechnol. Adv.* **29** 739–67

[3] Fujihara K, Kotaki M and Ramakrishna S 2005 Guided bone regeneration membrane made of polycaprolactone/calcium carbonate composite nano-fibers *Biomaterials* **26** 4139–47

[4] Ferrari A and Cecchini M 2011 Cells on patterns *Generating Micro and Nanopatterns on Polymeric Materials* (Germany: Weinheim) pp 267–90

[5] Yang F, Murugan R, Ramakrishna S, Wang X, Ma Y X and Wang S 2004 Fabrication of nano-structured porous PLLA scaffold intended for nerve tissue engineering *Biomaterials* **25** 1891–900

[6] Subramanian A, Krishnan U M and Sethuraman S 2011 Fabrication of uniaxially aligned 3D electrospun scaffolds for neural regeneration *Biomed. Mater.* **6** 025004

[7] Yoshii T, Dumas J E, Okawa A, Spengler D M and Guelcher S A 2011 Synthesis, characterization of calcium phosphates/polyurethane composites for weight bearing implants *J. Biomed. Mater. Res. Part* B **100B** 32–40

[8] Cheng M M C, Cuda G, Bunimovich Y L, Gaspari M, Heath J R, Hill H D, Mirkin C A, Nijdam A J, Terracciano R and Thundat T 2006 Nanotechnologies for biomolecular detection and medical diagnostics *Curr. Opin. Chem. Biol.* **10** 11–9

[9] Soleymani L, Fang Z, Sargent E H and Kelley S O 2009 Programming the detection limits of biosensors through controlled nanostructuring *Nature Nanotechnol.* **4** 844–8

[10] Devabhaktuni S and Prasad S 2009 Nanotextured organic light emitting diode based chemical sensor *J. Nanosci. Nanotechnol.* **9** 6299–306

[11] Dylewicz R, Khokhar A Z, Wasielewski R, Mazur P and Rahman F 2011 Nanotexturing of GaN light-emitting diode material through mask-less dry etching *Nanotechnology* **22** 055301

[12] Wan Y, Kim Y, Li N, Cho S K, Bachoo R, Ellington A D and Iqbal S M 2010 Surface-immobilized aptamers for cancer cell isolation and microscopic cytology *Cancer Res.* **70** 9371

[13] Wan Y, Mahmood M, Li N, Allen P B, Kim Y, Bachoo R, Ellington A D and Iqbal S M 2012 Nanotextured substrates with immobilized aptamers for cancer cell isolation and cytology *Cancer* **118** 1145–54

[14] Park T H and Shuler M L 2003 Integration of cell culture and microfabrication technology *Biotechnol. Progr.* **19** 243–53

[15] Yukna R A and Yukna C N 1998 A 5 year follow up of 16 patients treated with coralline calcium carbonate (Biocoral^{TM}) bone replacement grafts in infrabony defects* *J. Clin. Periodontol.* **25** 1036–40

[16] Velich N, Németh Z, Tóth C and Szabó G 2004 Long-term results with different bone substitutes used for sinus floor elevation *J. Craniofac. Surg.* **15** 38

[17] Coughlin M J, Grimes J S and Kennedy M P 2006 Coralline hydroxyapatite bone graft substitute in hindfoot surgery *Foot Ankle Int.* **27** 19
[18] Walsh W R, Morberg P, Yu Y, Yang J L, Haggard W, Sheath P C, Svehla M and Bruce W J M 2003 Response of a calcium sulfate bone graft substitute in a confined cancellous defect *Clin. Orthop. Relat. Res.* **406** 228
[19] Liao H, Mutvei H, Sjöström M, Hammarström L and Li J 2000 Tissue responses to natural aragonite (Margaritifera shell) implants *in vivo Biomaterials* **21** 457–68
[20] Borrelli J Jr, Prickett W D and Ricci W M 2003 Treatment of nonunions and osseous defects with bone graft and calcium sulfate *Clin. Orthop. Relat. Res.* **411** 245
[21] Bhumiratana S, Grayson W L, Castaneda A, Rockwood D N, Gil E S, Kaplan D L and Vunjak-Novakovic G 2011 Nucleation and growth of mineralized bone matrix on silk-hydroxyapatite composite scaffolds *Biomaterials* **32** 2812–20
[22] Siddharthan A, Sampath Kumar T S and Seshadri S K 2009 Synthesis and characterization of nanocrystalline apatites from eggshells at different Ca/P ratios *Biomed. Mater.* **4** 045010
[23] Siva Rama Krishna D, Siddharthan A, Seshadri S K and Sampath Kumar T S 2007 A novel route for synthesis of nanocrystalline hydroxyapatite from eggshell waste *J. Mater. Sci., Mater. Med.* **18** 1735–43
[24] Gergely G, Weber F, Lukacs I, Toth A L, Horvath Z E, Mihaly J and Balazsi C 2010 Preparation and characterization of hydroxyapatite from eggshell *Ceram. Int.* **36** 803–6
[25] Anderson J R, Chiu D T, Jackman R J, Cherniavskaya O, McDonald J C, Wu H, Whitesides S H and Whitesides G M 2000 Fabrication of topologically complex three-dimensional microfluidic systems in PDMS by rapid prototyping *Anal. Chem.* **72** 3158–64
[26] Duffy D C, McDonald J C, Schueller O J A and Whitesides G M 1998 Rapid prototyping of microfluidic systems in poly (dimethylsiloxane) *Anal. Chem.* **70** 4974–84
[27] Kahsai W T, Pham U H T, Sankaran J S and Iqbal S M 2012 Self-assembled synthesis and characterization of microchannels in polymeric membranes *J. Appl. Phys.* **112** 024701
[28] Dertinger S K W, Jiang X, Li Z, Murthy V N and Whitesides G M 2002 Gradients of substrate-bound laminin orient axonal specification of neurons *Proc. Natl Acad. Sci. USA* **99** 12542
[29] Leopold S, Kremin C, Ulbrich A, Krischok S and Hoffmann M 2011 Formation of silicon grass: nanomasking by carbon clusters in cyclic deep reactive ion etching *J. Vac. Sci. Technol.* B **29** 011002
[30] Jansen H, Boer M, Legtenberg R and Elwenspoek M 1995 The black silicon method: a universal method for determining the parameter setting of a fluorine-based reactive ion etcher in deep silicon trench etching with profile control *J. Micromech. Microeng.* **5** 115
[31] Nys Y, Gautron J, Garcia-Ruiz J M and Hincke M T 2004 Avian eggshell mineralization: biochemical and functional characterization of matrix proteins *C.R. Palevol* **3** 549–62
[32] Hunton P 2005 Research on eggshell structure and quality: an historical overview *Rev. Bras. Cienc. Avic.* **7** 67–71
[33] Tsai W T, Yang J M, Hsu H C, Lin C M, Lin K Y and Chiu C H 2008 Development and characterization of mesoporosity in eggshell ground by planetary ball milling *Microporous Mesoporous Mater.* **111** 379–86
[34] Tavangar A, Tan B and Venkatakrishnan K 2011 Synthesis of three-dimensional calcium carbonate nanofibrous structure from eggshell using femtosecond laser ablation *J. Nanobiotechnology* **9** 1
[35] Ślósarczyk A, Czechowska J, Paszkiewicz Z and Zima A 2010 New bone implant material with calcium sulfate and Ti modified hydroxyapatite *J. Achie. Mater. Manufact. Eng.* **43** 170–7
[36] Yang G Y, Bailey V J, Wen Y H, Lin G, Tang W C and Keyak J H 2004 Fabrication and characterization of microscale sensors for bone surface strain measurement *IEEE* **3** 1355–8
[37] Clark P, Connolly P, Curtis A S, Dow J A and Wilkinson C D 1991 Cell guidance by ultrafine topography *in vitro J. Cell Sci.* **99** 73